Li, Hui
Sun, Zhiyong
Han, Bingbing
Shao, Yuhang
Deng, Baoli

http://dx.doi.org/10.21278/brod73201 ISSN 0007-215X
eISSN 1845-5859

RESEARCH ON THE MOTION RESPONSE OF AQUACULTURE SHIP AND TANK SLOSHING UNDER ROLLING RESONANCE

UDC 629.5.017.22:629.5.017.162
Original scientific paper

Summary

The double-row and double-chamfered aquaculture tank is a special tank structure of the aquaculture ship. The tank sloshing of this structure is coupled with the hull motion, which has an important impact on the safety of the hull motion. In the present study, research on the tank sloshing and hull motion response of aquaculture ships was conducted based on the model seakeeping and tank sloshing tests in regular waves. The test results were compared with the numerical simulation results of solid loading without sloshing. The results showed that the numerical simulation of the pitch motion was consistent with the amplitude-frequency response curve of the experimental results. Under certain transverse wave conditions, a large discrepancy existed between the amplitude-frequency response curve of the heave motion by the numerical simulation and the test results, and the roll motion differed most from the experimental result. Severe roll resonance occurred when the wave length-ship length ratio was 0.6. The roll motion amplitude was increased by 183.2%. Therefore, compared with aquaculture ships without sloshing, the sloshing of the tank has little effect on the pitch but has a great impact on the roll and heave motions, with the most significant effect on the roll motion.

Key words: *Aquaculture ships; Tank sloshing; Ship motion; Roll resonance*

1. Introduction

As a new type of fishery aquaculture equipment, the aquaculture ship has great application prospects in the fishery aquaculture field. The hull motion response and tank sloshing during operation significantly impact fish growth. In addition, the slamming pressure caused by tank sloshing poses a threat to the safety of the bulkhead structure. Especially when roll resonance occurs under wave action, tank sloshing will further intensify the slamming effect of the water on the bulkhead. Therefore, the hull motion response and the law of tank sloshing in roll resonance are worthy of in-depth study.

In actual sea conditions, the aquaculture ship is affected by the combined effects of wind, waves, and currents, causing complex motion responses [1]. In recent years, researchers have mainly studied the motion response of general aquaculture equipment. A hydrodynamic experiment on a multi-module aquaculture platform conducted by Bi et al. revealed that nets

have a significant effect on the motion characteristics of the modules, and the influence of the nets on the damping of the heave motion is larger than that of the pitch motion [2]. Ma et al. simulated the hydrodynamic response of a single-point moored vessel-shaped floating aquaculture platform in waves using potential flow theory and dynamic composite cable theory [3]. Zhao et al. investigated the hydrodynamic response of semi-submersible offshore fish farms in waves through experiments and found that wave parameters, draught, and nets have a significant effect on the hydrodynamic response [4]. Liu et al. proposed a numerical model to analyze the hydrodynamic response of a semi-submersible aquaculture facility and studied the effects of wavelength and wave steepness on the mooring line tension and motion response [5]. Different from the general aquaculture facilities, in the aquaculture tank based on the enclosed hull, tank sloshing can greatly impact the response of the hull motion. At present, studies on tank sloshing have focused on barges or LNG ships [6,7,8]. However, unlike barges and LNG ships, the aquaculture ship has more double-row and double-chamfered aquaculture tanks. The problem of tank sloshing and hull motion response of aquaculture ships has attracted preliminary discussions among researchers. Based on the viscous flow theory, Wu et al. simulated the effect of tank sloshing on the motion response of an actual aquaculture ship under transverse wave conditions using overlapping grid technology [9]. Kong et al. investigated the influence of 12 aquaculture tanks on the hydrodynamic performance of roll and conducted a time-domain coupling analysis of the single-point mooring system. The results show that tank sloshing has a non-negligible effect on the hydrodynamic performance of the ship. After long periods of extreme working conditions, the ship will produce greater "fishtail motion" [10]. Gao et al. studied the influence of external incentives, sway control measures, and tank types on the rolling motion of the aquaculture ship through numerical simulation analysis methods and obtained the flow field structure and the law of anti-rolling action under different working conditions [11]. Using STAR-CCM commercial software, Cui et al. studied the flow field characteristics and wall pressure distribution of aquaculture tanks in pitch motion and established an evaluation method for the fishing suitability of aquaculture tanks [12]. Xiao et al. established a set of coupled numerical solution systems to solve excessive numerical calculation of tank sloshing of aquaculture ships and used the CFD method to study the coupling of multi-tank sloshing and hull motion [13, 14, 15]. Based on the three-dimensional potential flow theory, Han studied the seakeeping performance of aquaculture ships in the frequency domain and the time domain under self-propelled and mooring conditions, respectively [16]. The current research works on aquaculture ships are mostly based on commercial software simulations. However, due to the highly nonlinear effect, the theoretical analysis and numerical simulation of tank sloshing are imperfect, and the model test remains the most effective method to study tank sloshing [17, 18, 19].

Therefore, in this study, for a double-row and double-chamfered aquaculture tank structure, experimental research was conducted on the roll, pitch, heave motion response, and tank sloshing of the aquaculture ship in regular waves. The experimental results were compared with the hull motion response results of the same solid loading calculated by COMPASS-WALCS-BASIC software based on the three-dimensional potential flow theory. The effect of tank sloshing on the movement of the aquaculture ship was analyzed. Additionally, according to the roll resonance that appeared in the experiment, the CFD method was used to further study the physical phenomenon in the tank at resonance, and the causes of resonance were obtained.

2. Experimental equipment and methods

2.1 Ship model design

The test model is a 100,000-ton-class aquaculture ship designed by the China Fisheries Machinery Research Institute. The ship has 15 double chamfered diamond-shaped tanks. Except for the first tank in the bow, the rest tanks are arranged symmetrically in two rows. When fully loaded, the loading rate of the liquid tank is 78%. The layout of the actual ship's tanks is shown in Fig. 1. The section profile of the fourth tank is shown in Fig. 2.

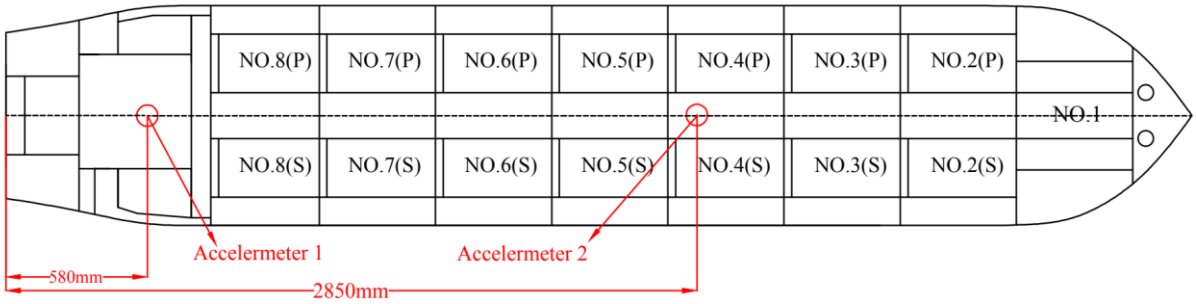

Fig. 1 Sectional drawing of tanks layout of aquaculture ship

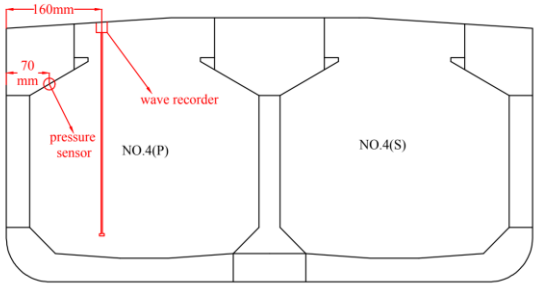

Fig. 2 Section profile of the fourth tank

Fig. 3 Ship model

The scale ratio of the model is selected as 1:50, and the ship model is made of glass fiber reinforced plastic with the consideration of the operability of the test and the conditions of the test tank. The thickness of the hull is 11mm. In order to ensure the hull has certain strength and the position of the tanks, two keels are arranged at the bottom of the ship, and a certain number of frames are arranged between the front and rear tanks. The model parameters and appearance shape are shown in Table 1 and Fig. 3.

Table 1 Ship model parameters

Designation	Signal	Ship	Model	Unit
Length overall	*L*	250.0	5.000	m
Breadth moulded	*B*	45.0	0.900	m
Depth	*H*	21.5	0.430	m
Center of gravity above base	*Zg*	11.6	0.232	m
Center of gravity form AP	*Xg*	126.2	2.524	m
Draft	*T*	12.0	0.240	m
Displacement	Δ	111250.0	0.868	t
Radius of roll gyration	*Rxx*	12.3	0.246	m
Radius of pitch gyration	*Ryy*	56.0	1.120	m
Radius of yaw gyration	*Rzz*	56.7	1.134	m

2.2 Experimental equipment

The test was carried out in the multifunctional tank (50 m long, 30 m wide, and 10 m deep) of Harbin Engineering University. The push plate wavemaker can produce regular and irregular waves at the specified frequency. In the experiment, Qualisys six-degree-of-freedom optical non-contact attitude measurement system was used to collect the movement data of the ship model. Besides, accelerometers were arranged at the midship and stern to monitor the acceleration response at different hull positions. The specific arrangement position is shown in Fig. 1. As shown in Fig.2, measuring points and wave altimeters are arranged in the 4th tank on the port side of the midship and the 8th tank on the starboard side of the stern to separately monitor the wall slamming pressure and liquid level rise caused by tank sloshing to better monitor the tank sloshing situation in the tanks.

2.3 RAO mooring

In order to fix the heading angle of the ship, four horizontal mooring lines were used to moor the test model. The mooring lines are composed of springs and thin steel wire ropes. The stiffness of the springs should not be too large to avoid large tensile force acting on the model. Because the vertical position of the model's center of gravity is lower than the model's draft, the four connection points of the mooring line on the model are chosen to be within the draft level [20]. The advantage of this mooring is that the model will not drift significantly under wave action, thus limiting the second-order low-frequency motion of the ship model in the waves, and will not affect the first-order high-frequency motion. The mooring arrangement of the ship model in the heading waves is shown in Fig. 4.

2.4 Experimental conditions

The working conditions of test are shown in Table 2. The 0° wave direction is the heading wave direction of the ship, and the 180° wave direction is the direction of the ship stern following the waves.

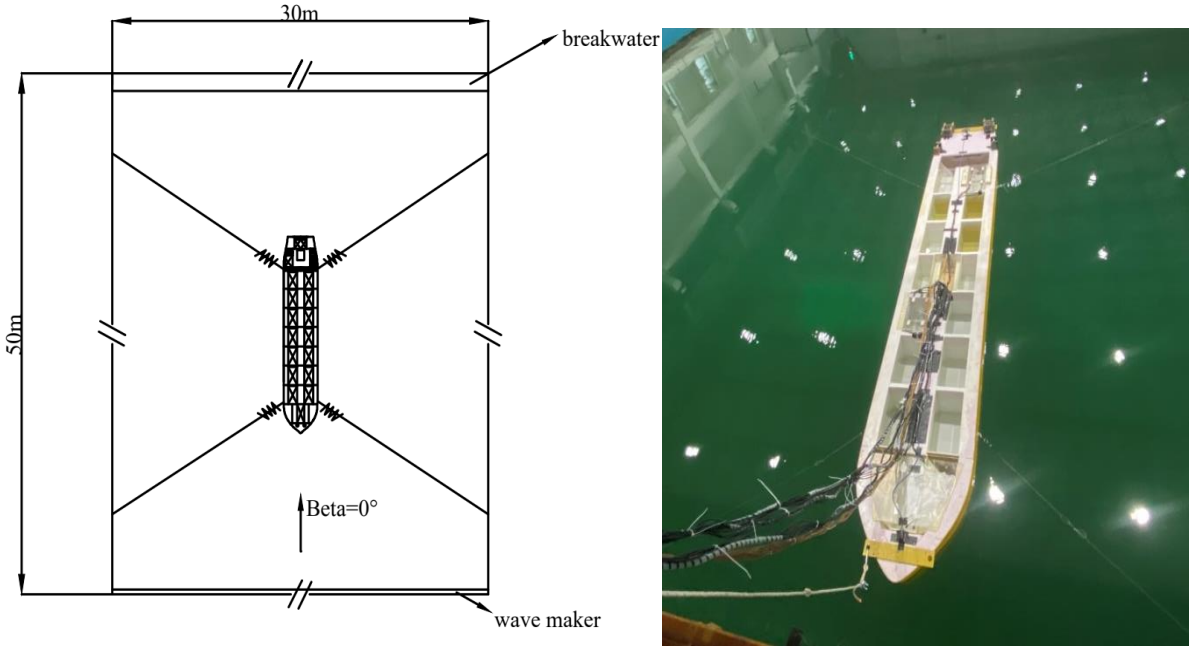

(a) (b)

Fig. 4 Mooring arrangement in heading waves

Table 2 Test conditions

Working condition	Wave direction θ	Wave height H	wave length-ship length ratio λ/L
R01-R09	0°	100mm	0.4,0.6, 0.8, 0.9, 1.0, 1.1, 1.2,1.5,2.0
R010-R18	45°	100mm	0.4,0.6, 0.8, 0.9, 1.0, 1.1, 1.2,1.5,2.0
R19-R27	90°	100mm	0.4,0.6, 0.8, 0.9, 1.0, 1.1, 1.2,1.5,2.0
R28-R36	135°	100mm	0.4,0.6, 0.8, 0.9, 1.0, 1.1, 1.2,1.5,2.0
R37-R45	180°	100mm	0.4,0.6, 0.8, 0.9, 1.0, 1.1, 1.2,1.5,2.0

3. Hydrodynamic modeling

The COMPASS-WALCS-BASIC software system based on the potential flow theory was used to calculate the hydrodynamic response of aquaculture ships with the same solid loading. The parametric modeling method was adopted, and the hull surface mesh was divided according to the hull line, as shown in Fig. 5. The floating state was adjusted according to the mass distribution of the hull. The resulting wet surface mesh is shown in Fig. 6, and calculation parameters of waves are shown in Table 3.

Fig. 5 Hull surface mesh

Fig. 6 Wet surface mesh

Table 3 Calculation parameters of waves

Calculation parameters	Parameter values
Wave conditions/(degree)	0, 45, 90, 135, 180
Frequency/(rad/s)	0.35, 0.40, 0.45, 0.50, 0.55, 0.60, 0.65, 0.70, 0.75, 0.80

4. Results and discussions

4.1 Roll attenuation experimental in still water

Figure 7 shows the time history curve of the roll attenuation of the model in still water. The total time of 10 rolling cycles was selected for average, and the natural period of roll of the ship model was calculated as 1.455 s, corresponding to the natural frequency of 4.318 rad/s. Solving the dimensionless attenuation coefficient directly from the attenuation curve was difficult because the roll damping and the roll angular velocity were not linear. Therefore, the elimination curve-$\Delta\varphi=f\left(\varphi_m\right)$ was introduced, and the critical damping coefficient of the roll was obtained by fitting a straight line to the elimination curve, where $\Delta\varphi=\varphi_k-\varphi_{k-1}, \varphi_m=\left(\varphi_k+\varphi_{k+1}\right)/2$ [21]. The dimensionless attenuation coefficient was calculated to be 0.102, and the roll damping coefficient was 0.051.

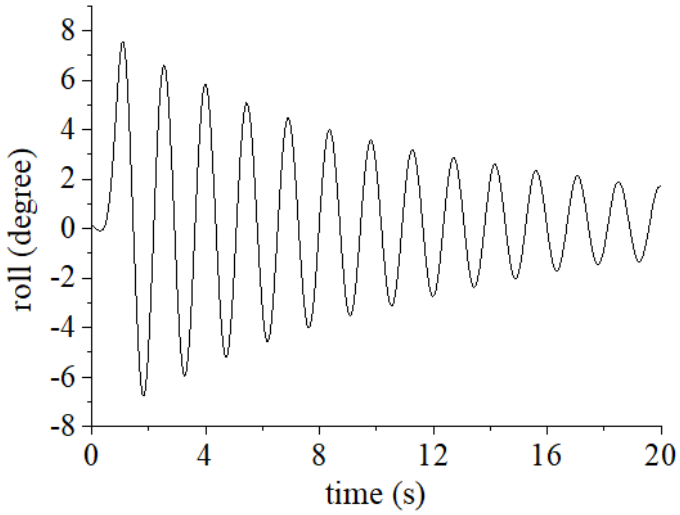

Fig. 7 Time history curve of roll attenuation

4.2 Comparison of motion response results

Figure 8 shows the contrast curve of amplitude and frequency response of the pitch. The experimental data and numerical simulation calculation show that the change form and value of the pitch amplitude-frequency response curve are similar. Due to the long length and small sloshing amplitude of the aquaculture tank in the pitch motion, the restoring force of pitch by the flow field was larger than the sloshing moment. The impact of tank sloshing on the restoring force was small. Therefore, the influence of tank sloshing on the pitch motion is small to negligible. Moreover, the numerical calculation results showed that the pitch curve exhibits double-peak characteristics under the conditions of heading waves. The first peak is around 0.45 rad/s, which is large; and the second peak is around 0.7 rad/s, which is small. The reason for the double peak phenomenon is that there is a sudden change in the wave interference force at ω =0.7 rad/s due to the hull shape, which leads to a peak of the pitch RAO at ω =0.7 rad/s in the heading wave. The test data curve cannot reflect the characteristics of the second peak because the test did not set the corresponding conditions at the wave length-ship length ratio of about 0.5.

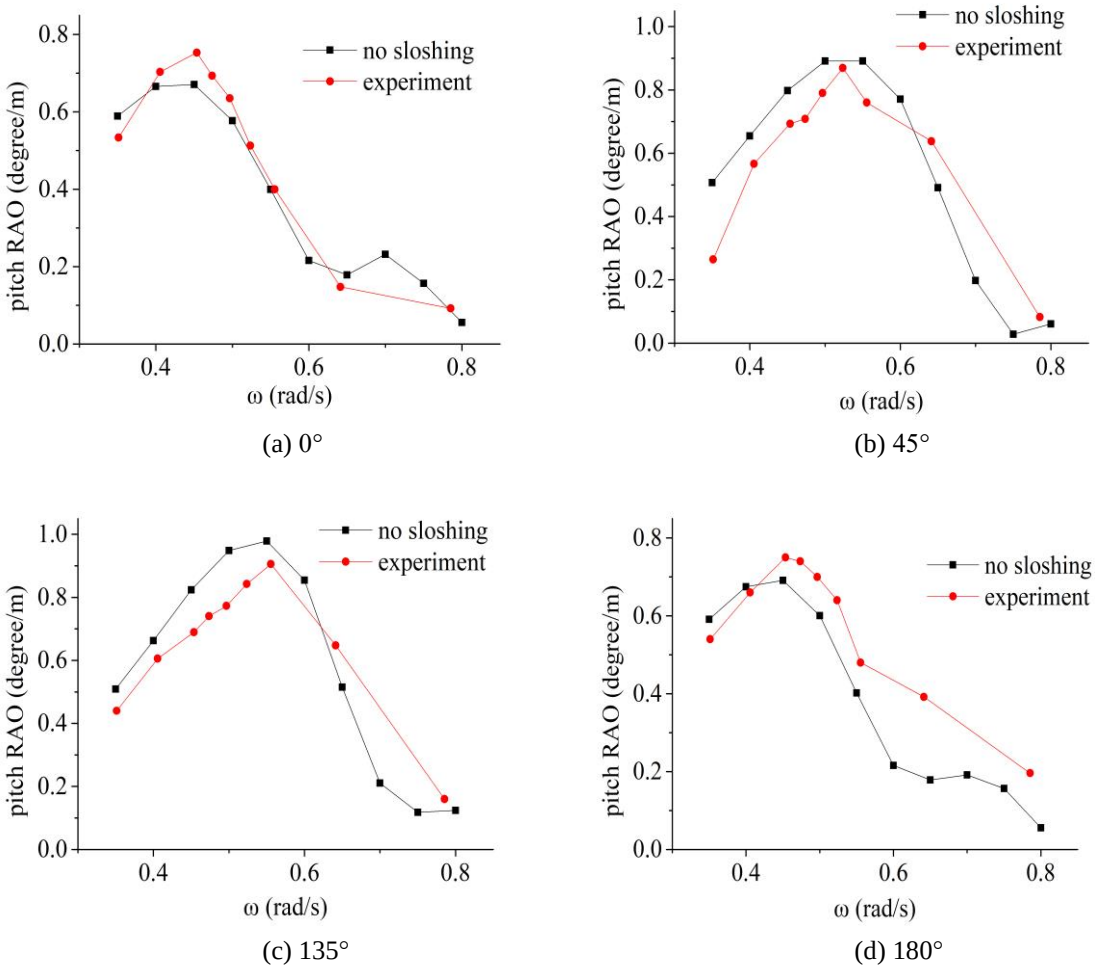

Fig. 8 Curves of the amplitude and frequency response of the pitch

The heave motion profile of the tank is approximately rectangular, so the first-order natural frequency of the tank heave is calculated as 1.17 rad/s according to the empirical formula of the rectangular tank [22]. Figure 9 shows the contrast curve of the amplitude and frequency response of the heave. The results of wave direction working conditions, except for the 90° wave direction, show similar changing shapes and values of the amplitude and frequency response curve of the heave. Since tank sloshing is less sensitive to the heave motion, and the restoring force of the flow field of the ship itself is larger than the sloshing force in the heave direction, the impact of tank sloshing on the heave motion is small. The experimental value and the numerical simulation result show a significant difference around ω=0.55 rad/s at the 90° wave direction. The Fourier transform was performed on the tank liquid level rise curve at the wave length-ship length ratio of 0.8 (Fig. 8). As shown in Fig. 8, the abscissa corresponding to the first peak is equal to the wave excitation frequency. The abscissa corresponding to the second peak is equal to the natural frequency of tank heave estimated by the empirical formula. When the amplitude of the heave motion is large, the resonance of the first-order frequency of the tank heave will be caused. The heave motion amplitude is further increased by the coupling of tank resonance and wave excitation. Therefore, the experimental value around ω=0.55 rad/s is quite different from the numerical calculation result.

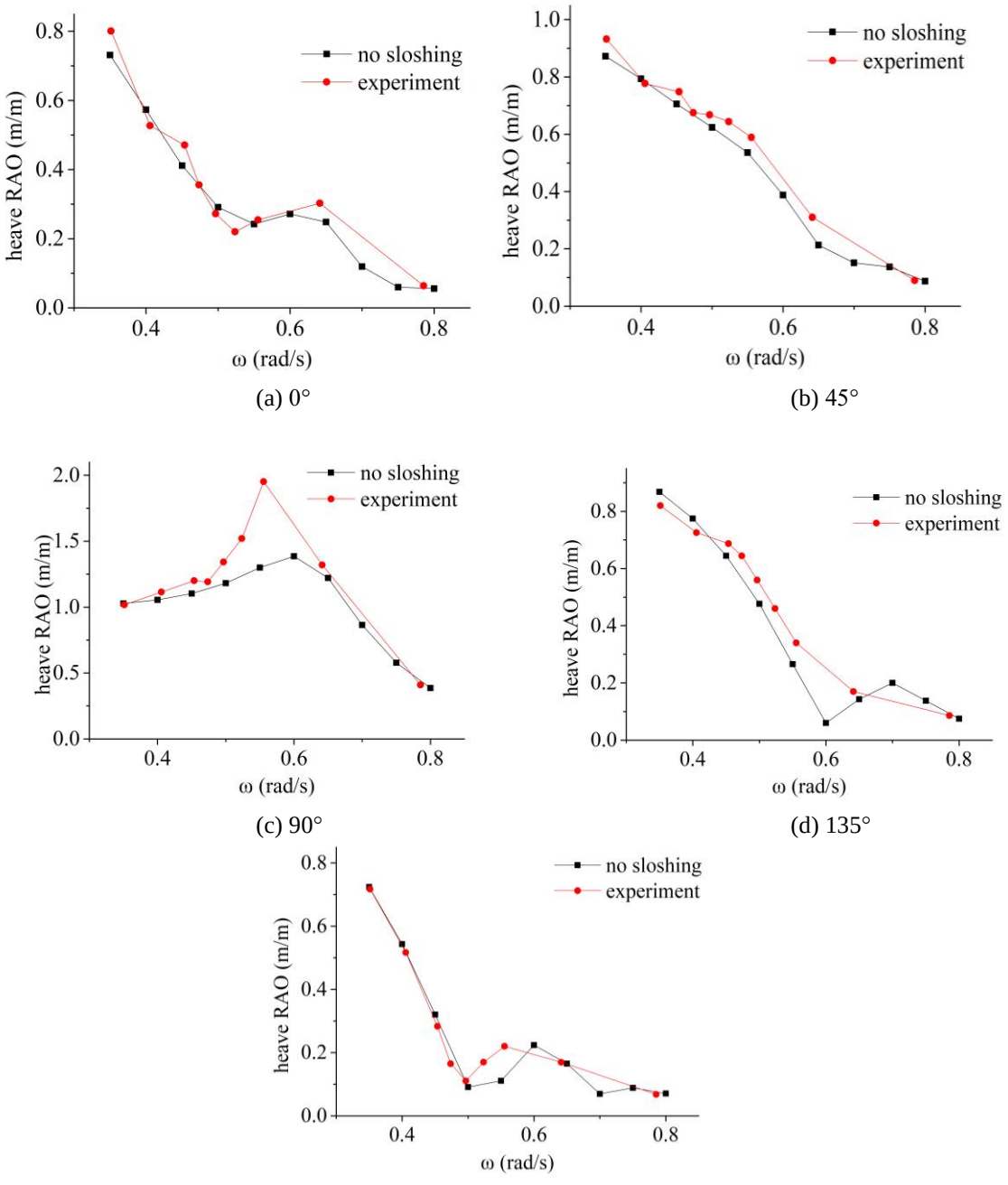

Fig. 9 Curves of the amplitude and frequency response of the heave

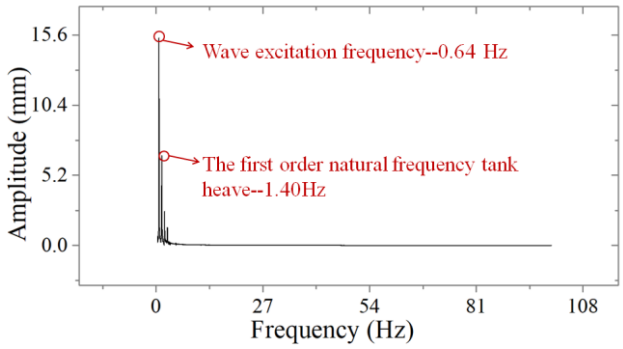

Fig. 10 Fourier change of tank wave surface rise

The contrast curves of the amplitude and frequency response of roll are shown in Fig. 11. The changing shape and value of the roll amplitude-frequency response curve are different, which is specifically manifested in the following two aspects:

(1) The peak value of the amplitude-frequency response curve is different. At 45° and 135° wave directions, the peak values of the test amplitude-frequency response curves are smaller than the simulated calculated value; the experimental values are reduced by 28.3% and 39.2%, respectively, compared with the numerical calculation results. At the 90° wave direction, the peak value of the test amplitude-frequency response curve is greater than the simulated calculation value. The test value increases by 183.2% compared with the numerical calculation result.

(2) The frequency corresponding to the peak of the amplitude-frequency response curve is different. The calculated value of the amplitude-frequency response curve reaches its peak at ω=0.5 rad/s, and the test value reaches its peak at ω=0.65 rad/s.

The width of the aquaculture tank is shorter than the length, and the roll amplitude of the ship is greater than the pitch amplitude. Therefore, the aquaculture water in the tank will slosh significantly along the width of the tank, and the sloshing moment is larger than the roll restoring moment. According to the comparison curves of 45°, 90°, 135° wave directions, the roll amplitude will be reduced due to the influence of tank sloshing at low frequency. Around the natural frequency of roll, the tank sloshing will further aggravate the rolling motion due to the violent sloshing motion of the tank. At the wave direction of 90°, when ω=0.65 rad/s, the wave frequency is close to the natural rolling frequency, leading to an obvious resonance phenomenon. The rolling motion of the hull is intensified, and the rolling motion amplitude is increased, causing violent sloshing in the tank. The sloshing moment acts on the hull, thus further intensifying the rolling motion.

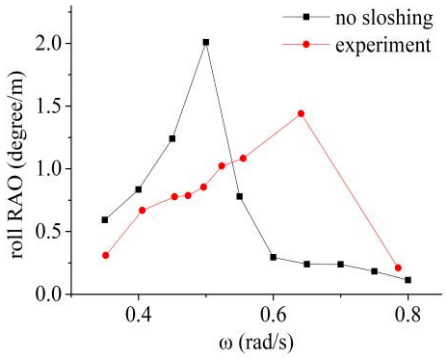

(a) 45°

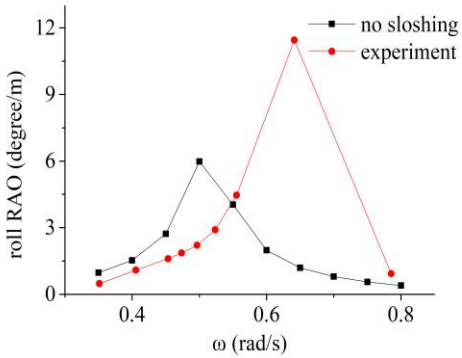

(b) 90°

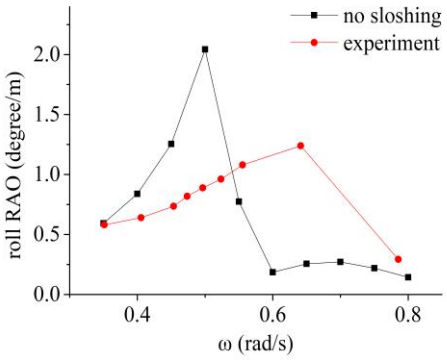

(c) 135°

Fig. 11 Curves of the amplitude and frequency response of roll

4.3 Research on sloshing phenomenon in rolling resonance

Aiming at the severe roll resonance in the test conditions where the wave direction is 90°, and the length ratio of the ship is 0.6 in the above studies, repeated test studies have been conducted to eliminate accidental errors in the test. Because the hull roll angle was too large under the wave height of 100 mm, the deck was flooded, and the ship model was close to the overturned state. Therefore, the test wave height in this working condition was modified to 50 mm. The acceleration of the hull motion, the rise of the wave surface in the tank, and the sloshing pressure of the bulkhead were monitored to describe the sloshing situation in the tank when the hull rolled resonance.

Fig. 12 shows the response state of the ship model at a certain moment when the ship rolls in resonance. The amplitude of the roll motion was large, causing the violent tank sloshing phenomenon in the aquaculture tanks. The surface of the aquaculture water in the tank was severely broken, and part of the aquaculture water even splashes above the deck. The hull was close to capsizing in the extreme state of roll.

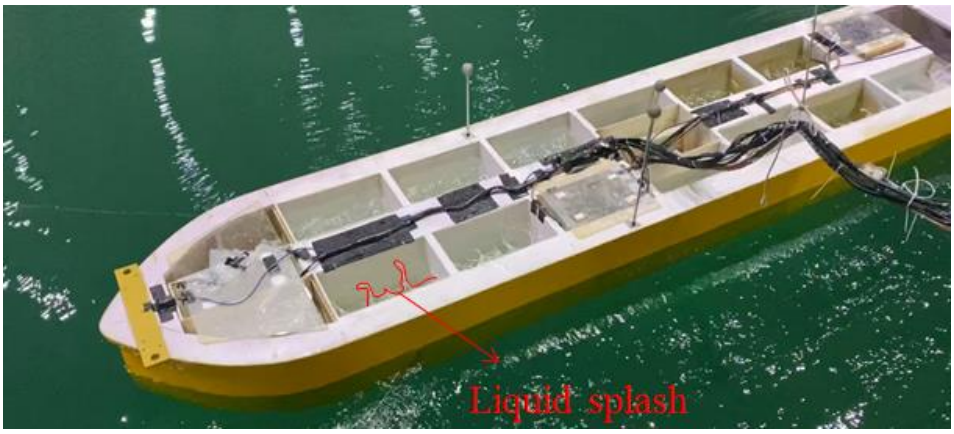

Fig. 12 Model response state during roll resonance

In order to intuitively display the sharp change of the tank sloshing parameters during the roll resonance, the data of the λ/L=0.8 working condition, which is closest to the wave length-ship length ratio of the resonance condition, was selected for comparison. Figure 13 (a) and Figure 13 (b) are the acceleration time history response curves of the midship and stern when λ/L=0.8 and λ/L=0.6, respectively. Figure 14 (a) and Figure 14 (b) are the sloshing pressure time history curves of the midship and stern tank when λ/L=0.8 and λ/L=0.6, respectively. Figure 15 (a) and Figure 15 (b) are the liquid level rise time history curves of the midship and stern tank when λ/L=0.8 and λ/L=0.6, respectively. The comparison of the test data of the two working conditions shows that the difference between the vertical acceleration curves is small. When λ/L=0.6, the acceleration of the stern tank is 16.5%, smaller than the acceleration of the stern tank when λ/L=0.8 because although rolling motion produces resonance, it has little effect on heave motion. The pressure and liquid level rise curves differ in the working conditions of λ/L=0.8 and λ/L=0.6. When λ/L=0.8, there is no obvious slamming pressure. When λ/L=0.6, there will be obvious slamming pressure. When λ/L=0.6, the hydrodynamic pressure of the stern tank is 139.1% larger than that when λ/L=0.8. When λ/L=0.6, the rise of stern tank liquid level is 191.5% larger than when λ/L=0.8. The results show that the pressure and the rise of the liquid level are sensitive to the amplitude of the roll motion, and the occurrence of roll resonance intensifies the amplitude of the roll.

As shown in Fig. 15(b), (c), the liquid level rise curve has three peaks in each sloshing cycle. The first maximum peak is the limiting water level caused by the hull motion, which is shown in Fig. 16(a). The second peak is generated because the wave surface slams violently on the other side of the inclined bulkhead after the first peak, forming a rollover wave, as

shown in Fig. 16(b). The formation of the third peak is due to the wave surface disturbance caused by the rolling wave, which can be seen in Fig. 16(c).

Since the bottom of the stern is relatively flat, there will be an obvious slamming phenomenon, causing the motion response of the stern tanks to be significantly greater than that of the midship tanks. Figure 14 (b) shows that the slamming phenomenon of the stern tank is obvious. There is obvious slamming pressure in each cycle, while the midship tank has a few slamming times and small slamming pressure peaks. From the overall trend of the slamming pressure of the two, the peak value of the slamming pressure varies greatly due to the violent rolling motion that causes the violent and irregular sloshing of the aquaculture water in the tank, leading to a strong non-linear slamming. Except for the slamming pressure, the trend and amplitude of the hydrodynamic pressure of the midship and stern tank are roughly the same because the hydrodynamic pressure is mainly related to the wave surface undulation in the tanks caused by the motion of the hull. The roll is dominant in the condition of 90° wave direction, and the amplitude of the bow and stern tanks is equal, then the hydrodynamic pressure changes in the same trend.

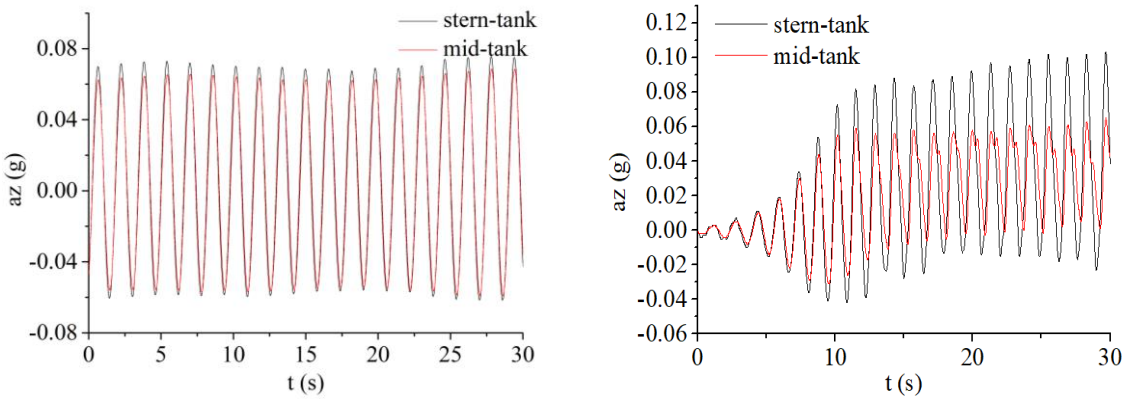

(a) λ/L=0.8 (b) λ/L=0.6

Fig. 13 Acceleration time history curve

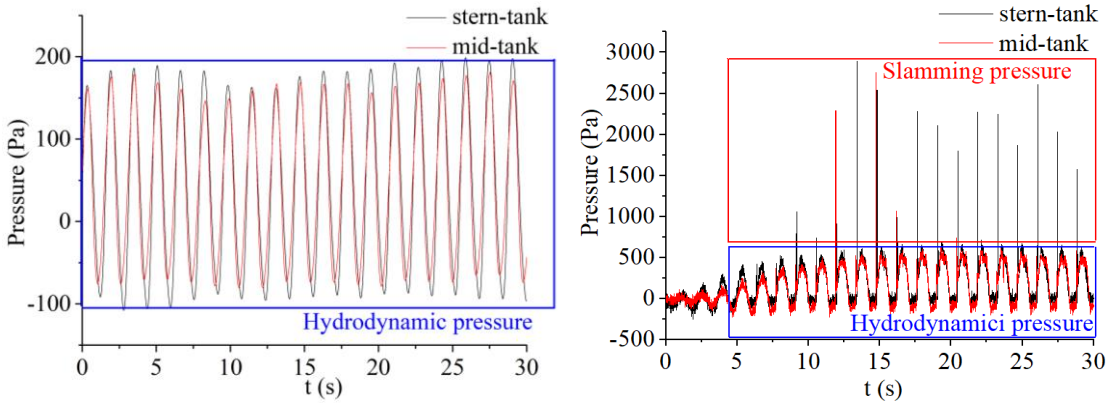

(a) λ/L=0.8 (b) λ/L=0.6

Fig. 14 Sloshing pressure time history curve

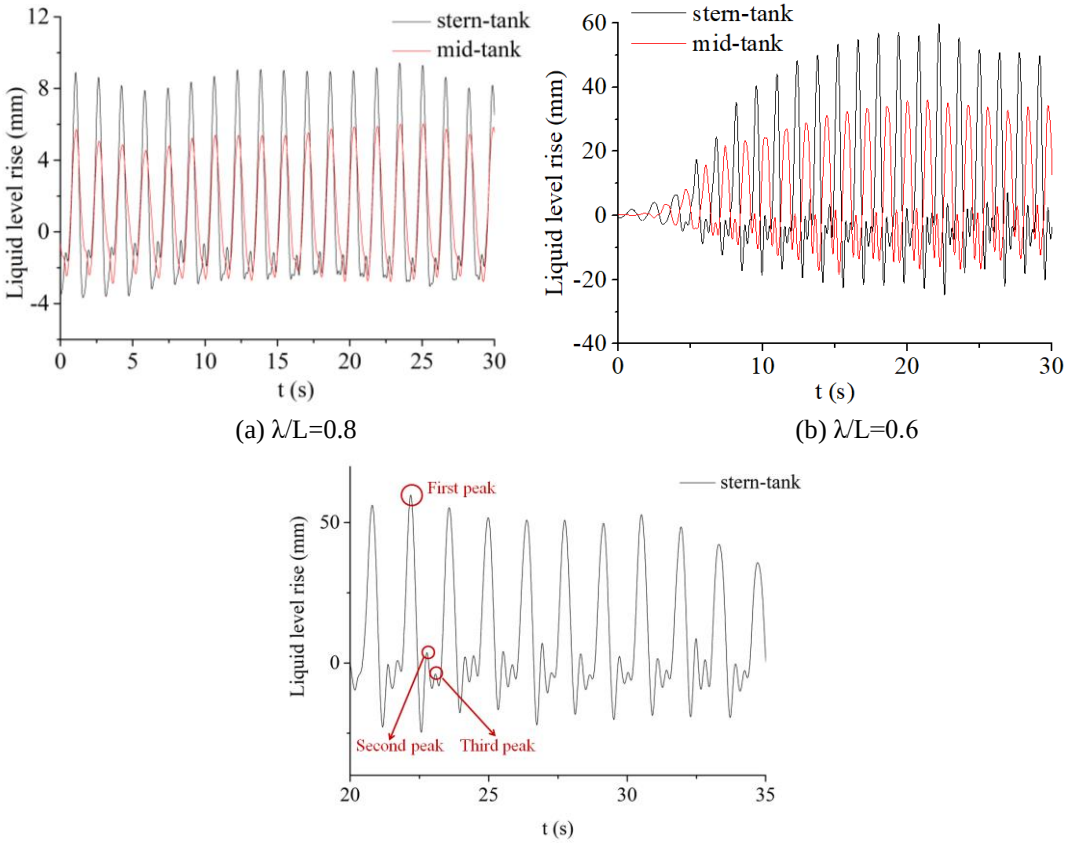

(a) λ/L=0.8 (b) λ/L=0.6

（c）λ/L=0.6 Local time history curve of stern-tank

Fig. 15 Liquid level rise time history curve

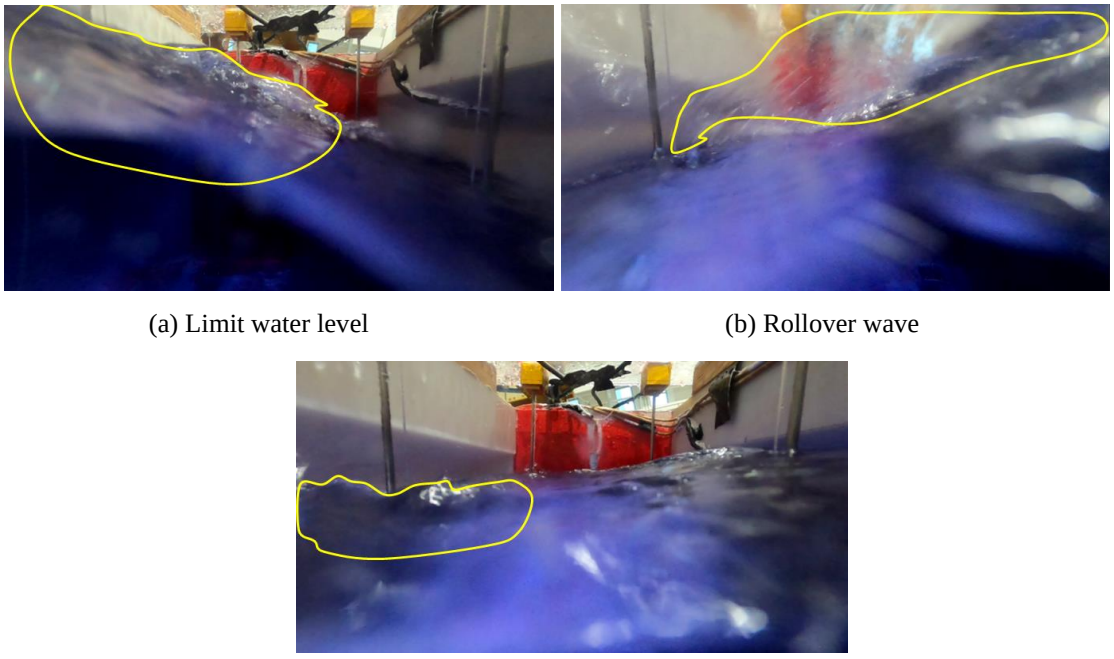

(a) Limit water level (b) Rollover wave

(c) Wave surface disturbance

Fig. 16 Video screenshot of liquid level in the tank

In order to study whether the resonance of this working condition was the resonance caused by the combination of wave frequency, hull roll natural frequency, and tank roll natural frequency, the first-order natural frequency of the model tank roll was studied. The

tanks of the aquaculture vessel were in the double-chamfered diamond tanks, which were quite different from rectangular tanks and single-chamfered diamond tanks. The existing rectangular tank and the improved formula for calculating the double-chamfered diamond tank have great limitations and are not suitable for calculating the tank's natural frequency [23]. Therefore, based on the CFD method, the STAR-CCM+ is used to search for the natural frequency of the tank rolling motion. Firstly, according to different water depths, multiple pressure measuring points are arranged on the long side bulkhead of the tank, the corner 1 and corner 2 positions, and the pressure values at various frequencies are calculated. According to the pressure curves at various measuring points in Fig. 18, the pressure value increases with the increase of the roll frequency. When ω= 5.2rad/s, the pressure value increases significantly. Therefore, ω=5.2rad/s is the first-order natural frequency of the tank's roll motion. The resonance frequency of the ship model when roll resonance occurs is 4.53, which is far away from the first-order natural frequency of the tank. The resonance under this working condition can exclude the influence of the tank roll resonance.

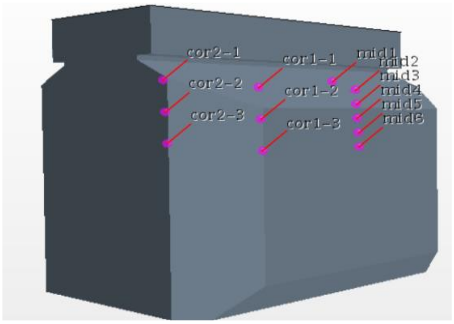

Fig. 17 Measuring points layout

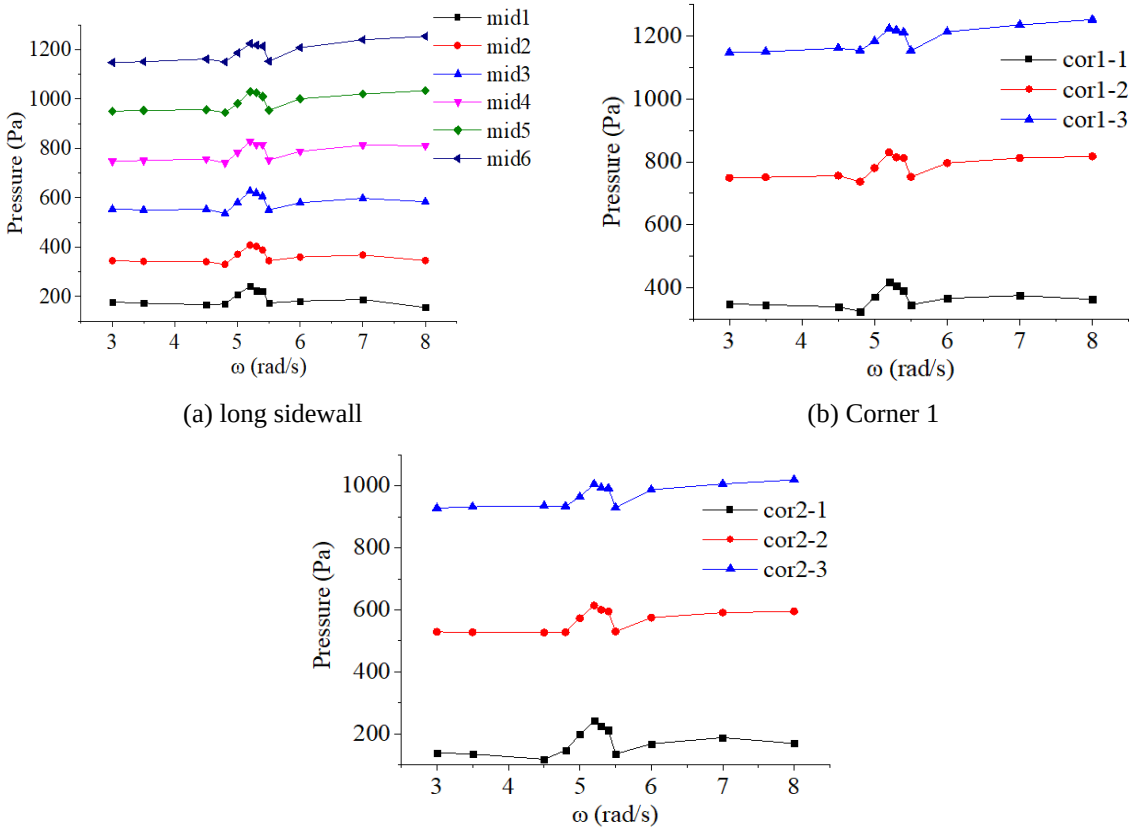

(a) long sidewall

(b) Corner 1

(c) Corner 2

Fig. 18 measuring point pressure value

5. Conclusions

In this paper, the model test of seakeeping and tank sloshing was conducted for an aquaculture ship with a double-row and double-chamfered aquaculture tank, and the heave, pitch, and roll motions of the ship hull in five regular wave directions were studied. The test results were compared with the numerical calculation data of the model with the same solid load, and the roll resonance that occurred in the test was studied. The main conclusions are as follows:

(1) In the pitch motion, the excitation of the hull motion is small, so the tank sloshing amplitude is small. The restoring force of the ship itself by the flow field is large, and tank sloshing has little effect on the restoring force. Therefore, the influence of tank sloshing of aquaculture ships with double-row and double-chamfered aquaculture tanks on the pitch motion is small.

(2) In the heave motion, when the heave amplitude is small, the sloshing moment is smaller than the heave restoring moment. Thus, the tank sloshing has little effect on the heave motion of the aquaculture ship; when the heave amplitude is large, the first-order resonance of the tank heave will be coupled with the hull motion, thereby intensifying the heave motion.

(3) In the rolling motion, the amplitude of the rolling motion is large, and the sloshing moment is large relative to the roll restoring moment, so the sloshing of the tank has the greatest influence on the roll motion. The sloshing of the tank at low frequencies can suppress the rolling motion. Around the natural frequency of hull roll, the intense sloshing of the tank will intensify the roll motion of the hull.

Acknowledgments

This work was financially supported by the National Natural Science Foundation of China (No. 52071110); Natural Science Foundation of Heilongjiang Province of China (No. LH2020E077); Key Research and Development Program of Shandong province (No. 2020CXGC010702).

REFERENCES

[1] Wu, W., Zhen, C., Lu, J., Tu, J., Zhang, J., Yang, Y., Duan, J., 2020. Experimental study on characteristic of sloshing impact load in elastic tank with low and partial filling under rolling coupled pitching. *International Journal of Naval Architecture and Ocean Engineering*, 12, 178-183.

[2] Bi, C. W., Ma, C., Zhao, Y. P., Xin, L. X., 2021. Physical model experimental study on the motion responses of a multi-module aquaculture platform. *Ocean Engineering*, 239, 109862.

[3] Ma, C., Zhao, Y. P., Bi, C. W., 2022. Numerical study on hydrodynamic responses of a single-point moored vessel-shaped floating aquaculture platform in waves. *Aquacultural Engineering*, 96, 102216.

[4] Zhao, Y., Guan, C., Bi, C., Liu, H., Cui, Y., 2019. Experimental investigations on hydrodynamic responses of a semi-submersible offshore fish farm in waves. *Journal of Marine Science and Engineering*, 7(7), 238.

[5] Liu, H. F., Bi, C. W., Zhao, Y. P., 2020. Experimental and numerical study of the hydrodynamic characteristics of a semisubmersible aquaculture facility in waves. *Ocean Engineering*, 214, 107714.

[6] Panigrahy, P. K., Saha, U. K., Maity, D., 2009. Experimental studies on sloshing behavior due to horizontal movement of liquids in baffled tanks. *Ocean engineering*, 36(3-4), 213-222.

[7] Malenica, Š., Kwon, S. H., 2013. An overview of the hydro-structure interactions during sloshing impacts in the tanks of LNG carriers. *Brodogradnja*, 64(1), 22-30.

[8] Lee, S. B., Kim, H. Y., Park, J. S., Kwon, S. H., 2014. A study on the two-row effect in the sloshing phenomenon. *Transactions of FAMENA*, 38(4), 29-42.

[9] Wu, J., Chen, Z., 2021. Coupled motion of tank sloshing and aquaculture platform in regular beam sea, *Ship Engineering*, 43(4),17-23+47.

[10] Kong, Y., Chen, Z., 2021. Hydrodynamics and Single-Point Mooring Characterristic of Deep-Sea Tank Breeding Aquacture Platform. *Ship Engineering*, 43(4), 6-11.

[11] Gao, D., Cui, M., Wang, Q., et al., 2020. Numerical Analysis on Roll Fish-suitability of Aquaculture Water Tank. *Ship Engineering*, 42(12), 35-42+47.

[12] Cui, M., Wang, J., Guo. X., 2020. Numerical analysis of fish adaptability to roll in aquaculture tank. *Shipbuilding of China*, 61(03), 204-215.

[13] Xiao, K., Chen, Z., Dai, Y., 2020. Numerical Study on Coupling Effect of Multi-tank Sloshing and Ship Motion. *Ship Engineering*, 42(08), 50-54.

[14] Xiao, K., Chen, Z., 2020. Numerical simulation of aquaculture ship motions coupled with tanks sloshing in time domain. *Chinese Journal of Ship Research*, 15(1), 136-144.

[15] Xiao, K., 2020. Coupling analysis of tank sloshing and hull motion of deep sea aquaculture ship. Shanghai Jiaotong University, Shanghai.

[16] Han, B., Zhan, Z., Cui, M., Wang, Q., Wang, Y., Gao, R., 2020. Seakeeping Performance Analysis of Deep-sea Aquaculture Platform Based on the Three-dimensional Potential Flow Theory. *Fishery Modernization*, 47(6), 58-65.

[17] Xue M., 2011. Experimental Study of Liquid Sloshing in a Tank under Irregular Wave Excitation. *Proceedings of the 34th World Congress of the International Association for Hydro-Environment Research and Engineering: 33rd Hydrology and Water Resources Symposium and 10th Conference on Hydraulics in Water Engineering*, Brisbane, Australia.

[18] Nasar, T., Sannasiraj, S. A., Sundar V., 2008. Experimental study of liquid sloshing dynamics in a barge carrying tank. *Fluid Dynamics Research*, 40(6), 427-458.

[19] Martić, I., Degiuli, N., Ćatipović, I., 2016. Evaluation of the added resistance and ship motions coupled with sloshing using potential flow theory. *Brodogradnja*, 67(4), 109-122.

[20] Zhang, K., 2016. The Research of FPSO Bow Line under Single Point Mooring System. *Harbin Engineering University*, Harbin.

[21] Li, J., 1992. Ship Seakeeping. *Harbin Engineering University Press*, Harbin, China.

[22] Faltinsen, O.M., Timokha, A. N., 2009. Sloshing. *Cambridge University Press*, New York, USA.

Submitted: 09.03.2022.
Accepted: 18.03.2022.

Li, Hui *, szy472665629@163.com
Sun Zhiyong,
Han Bingbing
Shao Yuhang
Deng Baoli
College of Shipbuilding Engineering, Harbin Engineering University, Harbin, 150001, China